



HAL
open science

Theory for planetary exospheres: III. Radiation pressure effect on the Circular Restricted Three Body Problem and its implication on planetary atmospheres

A. Beth, P. Garnier, D. Toublanc, I. Dandouras, C. Mazelle

► To cite this version:

A. Beth, P. Garnier, D. Toublanc, I. Dandouras, C. Mazelle. Theory for planetary exospheres: III. Radiation pressure effect on the Circular Restricted Three Body Problem and its implication on planetary atmospheres. *Icarus*, 2016, 280, pp.415-423. 10.1016/j.icarus.2016.06.028 . insu-03669395

HAL Id: insu-03669395

<https://insu.hal.science/insu-03669395>

Submitted on 16 May 2022

HAL is a multi-disciplinary open access archive for the deposit and dissemination of scientific research documents, whether they are published or not. The documents may come from teaching and research institutions in France or abroad, or from public or private research centers.

L'archive ouverte pluridisciplinaire **HAL**, est destinée au dépôt et à la diffusion de documents scientifiques de niveau recherche, publiés ou non, émanant des établissements d'enseignement et de recherche français ou étrangers, des laboratoires publics ou privés.



Distributed under a Creative Commons Attribution 4.0 International License



Theory for planetary exospheres: III. Radiation pressure effect on the Circular Restricted Three Body Problem and its implication on planetary atmospheres



A. Beth^{a,b,c,*}, P. Garnier^{b,c}, D. Toublanc^{b,c}, I. Dandouras^{b,c}, C. Mazelle^{b,c}

^a Department of Physics, Imperial College London, Prince Consort Road, London SW7 2AZ, United Kingdom

^b Université de Toulouse, UPS-OMP, IRAP, Toulouse, France

^c CNRS, IRAP, 9 Av. colonel Roche, BP 44346, F-31028 Toulouse cedex 4, France

ARTICLE INFO

Article history:

Received 3 August 2015

Revised 1 April 2016

Accepted 30 June 2016

Available online 9 July 2016

Keywords:

Atmosphere, dynamics

Celestial mechanics

Solar radiation

Extra-solar planets

ABSTRACT

The planetary exospheres are poorly known in their outer parts, since the neutral densities are low compared with the instruments detection capabilities. The exospheric models are thus often the main source of information at such high altitudes. We present a new way to take into account analytically the additional effect of the stellar radiation pressure on planetary exospheres. In a series of papers, we present with a Hamiltonian approach the effect of the radiation pressure on dynamical trajectories, density profiles and escaping thermal flux. Our work is a generalization of the study by Bishop and Chamberlain [1989] *Icarus*, 81, 145–163. In this third paper, we investigate the effect of the stellar radiation pressure on the Circular Restricted Three Body Problem (CR3BP), called also the photogravitational CR3BP, and its implication on the escape and the stability of planetary exospheres, especially for hot Jupiters. In particular, we describe the transformation of the equipotentials and the location of the Lagrange points, and we provide a modified equation for the Hill sphere radius that includes the influence of the radiation pressure. Finally, an application to the hot Jupiter HD 209458b and hot Neptune GJ 436b reveals the existence of a blow-off escape regime induced by the stellar radiation pressure.

© 2016 The Authors. Published by Elsevier Inc.

This is an open access article under the CC BY license (<http://creativecommons.org/licenses/by/4.0/>).

1. Introduction

The exosphere is the upper layer of any planetary atmosphere: it is a quasi-collisionless medium where the particle trajectories are more dominated by gravity than by collisions. Above the exobase, the lower limit of the exosphere, the Knudsen number Kn (Ferziger and Kaper, 1972), defined as the ratio between the mean free path and the scale height, becomes larger than 1, the collisions become scarce, the distribution function cannot be considered as maxwellian anymore and, gradually, the trajectories of particles are essentially determined by the planetary gravity and radiation pressure by the Sun. The trajectories of particles, subject to the gravitational force, are completely solved with the equations of motion, but it is not the case with the radiation pressure (Bishop and Chamberlain, 1989) until recently.

The radiation pressure disturbs the conics (ellipses or hyperbolas) described by the particles under the influence of gravity. The

resonant scattering of solar photons leads to a total momentum transfer from the photon to the atom or molecule (Burns et al., 1979). In the non-relativistic case, assuming an isotropic reemission of the solar photon, this one is absorbed in the Sun direction and scattered with the same probability in all directions. For a sufficient flux of photons in the absorption wavelength range, the reemission in average does not induce any momentum transfer from the atom/molecule to the photon. The momentum variation, each second, between before and after the scattering imparts a force, the radiation pressure.

Bishop and Chamberlain (1989) analyzed its effect on the structure of planetary exospheres. Nevertheless, their work was limited only to the Sun-planet axis, with a null component assumed for the angular momentum around the Sun-planet axis. We thus generalize here their work to a full 3D calculation, in order to investigate the influence of the radiation pressure on the trajectories (Beth et al., 2016a), as well as the density profiles (Beth et al., 2016b) and escape flux (future work).

In this paper, we propose to investigate the influence of the radiation pressure on the stability of planetary exospheres, based on the dynamical effects of the radiation pressure. In particular, we study the validity of our approach (see Beth et al., 2016a;b) for

* Corresponding author at: Department of Physics, Imperial College London, Prince Consort Road, London SW7 2AZ, United Kingdom.

E-mail addresses: arnaud.beth@gmail.com (A. Beth), pgarnier@irap.omp.eu (P. Garnier).

the specific case of hot Jupiters and hot Neptunes, which needs to consider the Circular Restricted Three Body Problem (CR3BP) combined with the radiation pressure i.e. the photogravitational Three Body Problem. We will also derive a new expression of the Hill sphere radius (the limit of the gravitational influence of the central body) that includes the effect of the radiation pressure, before we discuss the impact of the radiation pressure force on the stability of the exoplanetary atmospheres (with a case study on HD 209458b and on GJ 436b). Indeed, these may be bounded or not to the planet depending on the radiation pressure intensity.

In Section 2, we develop our approach to study the photogravitational CR3BP. Then, in Section 3, we will present the topology of equipotentials, derive a new expression of the Hill sphere, compare with previous works and then discuss the possible consequence for the planetary atmosphere stability and the escaping flux. Moreover, we detail in Section 4 the set of assumptions made in his paper and discuss about their reliability. Finally, the conclusions will be reported in Section 5.

2. Formalism

We investigate here the combined effects of the external forces on planetary neutral exospheres: the planetary gravity, the stellar gravity, the centrifugal force and the radiation pressure. As we know, the radiation pressure is depending on the flux of photons and the relative speed towards/outwards the star. Indeed, because of the relativistic effects, the wavelength of the photon perceived by the species is slightly blue/red-shifted from the most efficient absorption wavelength in its rest frame. The Doppler-effect could be relatively important for narrow emission lines such as the Lyman- α line and atomic Hydrogen. Consequently, the radiation pressure should not be considered as a conservative force (depending on the velocity). Thereafter, we neglect relativistic effects such as the Doppler shift or the Poynting–Robertson effect as first approximation to conclude on the main consequences of the radiation pressure effect, so that this problem could be handled with a classical approach. Moreover, we do not consider the shadowing effect of the planet and its atmosphere which should mostly decrease the radiation pressure acceleration in the wake of the planet, particularly strong for the case of hot Jupiters (Bourrier and Lecavelier des Etangs, 2013). A more detailed discussion on the validity of these assumptions is provided in Section 4.

According to these assumptions, the radiation pressure then depends only on the square of the distance from the star as the stellar gravity. We define the β parameter as the ratio between the acceleration induced by the radiation pressure and by the stellar gravity, this parameter assumed to be a constant in the planetary system under the previous assumptions. Indeed, the radiation pressure effect without relativistic effects depends only on the flux and thus the square of the stellar distance as the stellar gravity.

Each species is then subject to the dimensionless effective potential $-\Omega(x, y, z)$ in the rotating coordinate system defined as:

$$\Omega(x, y, z) = \frac{1}{2}(x^2 + y^2) + \frac{(1-\beta)(1-\mu)}{r_S} + \frac{\mu}{r_{pl}} \quad (1)$$

and

$$\begin{cases} r_S = \sqrt{(x + \mu)^2 + y^2 + z^2} \\ r_{pl} = \sqrt{(x + \mu - 1)^2 + y^2 + z^2} \end{cases}$$

with $\mu = M_1/(M_1 + M_2)$, M_1 the mass of the planet, M_2 the mass of the star, $(-\mu, 0, 0)$ the position of the star and $(1 - \mu, 0, 0)$ the one of the planet. The axis are oriented such as the x -axis is the star-planet axis, the z -axis is perpendicular to the planetary motion and the y -axis so that the $Oxyz$ frame is a direct orthonormal basis. The notations are similar to the ones used in Simmons et al. (1985).

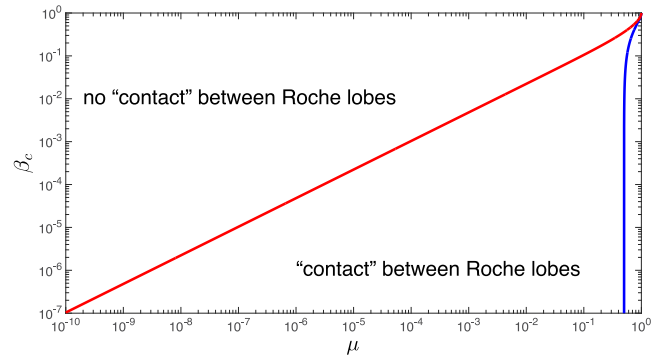


Fig. 1. Plots of critical β values adapted from Schuerman (1972) in log-scale, more adapted for our approach. The red curve represents the β_c value for which L_1 and L_2 share the same energy and thus the same equipotential. The blue plot is similar but applied between L_1 and L_3 and can exist only for $\mu > 0.5$ (this does not make sense for us because this means that the planet is heavier than the star). We retrieve the asymptotic behavior derived by Schuerman (1972) for $\mu = o(1)$: $\beta_c \sim (\mu/3)^{2/3}$. (For interpretation of the references to color in this figure legend, the reader is referred to the web version of this article.)

The first term of Ω describes the potential energy associated to the centrifugal force, the second one corresponds to the stellar gravity and the radiation pressure effect β , and the last one the planetary gravity.

This problem was previously studied concerning the positions and the stability of equilibrium points by Schuerman ([1972,1980]) and Simmons et al. (1985) in the case of a binary star system with a radiation pressure effect from both. Schuerman (1972) determined the analytical position of the Lagrange points L_4 and L_5 given by:

$$\begin{cases} r_S^3(L_4, L_5) = 1 - \beta \\ r_{pl}^3(L_4, L_5) = 1 \end{cases} \Rightarrow \begin{cases} x_{L_4, L_5} = (1 - \mu) - \frac{(1 - \beta)^{2/3}}{2} \\ y_{L_4, L_5} = \pm \sqrt[3]{1 - \beta} \sqrt{1 - \frac{(1 - \beta)^{2/3}}{4}} \end{cases}$$

where $r_S(L_4, L_5)$ and $r_{pl}(L_4, L_5)$ are the respective distances to the star and the planet. Moreover, they investigated the equipotentials and the β values for which the Roche lobe of the planet is connected to the stellar one through L_1 as a function of μ (our definition is slightly different) and β . For critical values of β , β_c (or δ_c in his paper), both are not connected at all (cf. Schuerman, 1972, Fig. 4): there is no “contact surface” any more (cf. Fig. 1).

On the other hand, Simmons et al. (1985) investigated the general case of a binary star system, where both stars have its own radiation pressure. They gave a complete review about the Lagrange points L_1 , L_2 and L_3 with the algebraic analysis of a five degree polynomial, whose roots are the Lagrange points positions, their numerical values and their stability. However, L_4 and L_5 were mostly studied by Schuerman (1980). A more recent study by Phillips and Podsiadlowski (2002) on binary systems investigated on the deformation of equipotentials and thus the stellar surface by the strong X-Ray emission from the companion, taking into account the optical depth within the star: this is similar to the planet-star system with the atmosphere of the planet; however, the range of masses are clearly different.

The link between the stability of a planetary atmosphere and the CR3BP was tackled by Lecavelier des Etangs et al. (2004) about the strong escape rate observed on HD 209458b and widely covered in the literature (Lecavelier des Etangs et al., 2004; Koskinen et al., 2013; Vidal-Madjar et al., 2003) and reviewed by Yelle et al. (2008). They modeled with different densities and

temperatures estimations the upper atmosphere of HD 209458b. For high thermospheric temperatures, the thermosphere could extend so far that the exobase could reach the Roche lobe limit, located at only ~ 4 planetary radii. Thus, in this case the requisite kinetic energy to escape from the exobase (or critical radius r_c) is smaller than the common gravitational potential GM_1/r_c . Several papers dedicated to HD 209458b investigated this issue, focusing on the mass loss rate and the conversion of the EUV flux into kinetic energy for Hydrogen so that it can escape. However, most of the previous studies deal with the tidal effects (Erkaev et al., 2007; Garcá Muñoz, 2007) but did not take into account the additional effect of the radiation pressure (i.e. $\beta \neq 0$) which acts as a strong repulsive force from the star on Hydrogen, the main atmospheric species especially for hot Jupiters or other planets at high altitudes.

In this paper, we first derive an analytical formula to approximate the Hill sphere radius with the additional effect of the radiation pressure which was never done before. Then, we will discuss the positions of the equilibrium points compared with the size of the extended planetary atmospheres and show how the radiation pressure will influence the stability of the atmospheres of exoplanets, with using HD 209458b and GJ 436b as two case studies.

3. Results

In this section, we present our results on the topology (3.1) and on the decreasing size of the Hill sphere due to the radiation pressure. We derive an analytical formula to approximate the Hill sphere size depending on the radiation pressure intensity (3.2). We will then discuss the implications of the modified Hill sphere on the planetary atmosphere stability (3.3). This modification will significantly affect the giant planets close to their host star such as hot Jupiters and hot Neptunes. This section will provide quantitative results for specific situations including the case of HD 209458b and GJ 436b (and for hydrogen atoms), but both the approach and the results can be essentially applied to any planetary atmosphere.

3.1. Topology of equipotentials

In this first part, we study the topology of equipotentials (or Zero-Velocity Curves ZVC) modified by the radiation pressure with the example of HD 209458b.

Figs. 2 and 3 show the topology of the equipotentials for increasing β values in the case of HD 209458b (i.e. $\mu \approx 5.73 \cdot 10^{-4}$, see http://exoplanet.eu/catalog/hd_209458_b/, Southworth, 2010; Wang and Ford, 2011 for the planet and star characteristics). Extremely close to its star (0.047 A.U.), with a mass (0.69 M_J) and a size (1.35 R_J) of the same order as Jupiter's ones, HD 209458b is strongly affected by tidal forces (Lecavelier des Etangs et al., 2004). Nevertheless, the photogravitational Three Body Problem was not yet covered concerning its implication on the stability of planetary exospheres; only the potential effects of tidal forces were investigated (Erkaev et al., 2007). We considered here a range of β values of 0 to 5, to be compared with the ranges of β values for Hydrogen at HD 209458b as reported by Bourrier and Lecavelier des Etangs (2013) (these authors take into account the Doppler shift so that β depends on the velocity along the radial direction with respect to the star, $\beta(v \approx 0) \approx 4$).

As can be seen in Figs. 2 and 3, the different Lagrange points migrate in the direction toward the star. Indeed, the radiation pressure is a force opposed to the stellar gravity. For increasing β values, the equilibrium points need to be nearer to the star in order to put up the radiation pressure acceleration.

For the critical value $\beta = 1$, all Lagrangian points disappear except L_2 which should stay behind the planet. However, for any β ,

L_2 becomes closer to the planet, and thus the sphere of influence or the Hill sphere has a decreasing size as a function of β .

In order to estimate the influence of β on the Hill sphere size, we derive in the next section a new Hill sphere radius taking into account the radiation pressure.

3.2. Hill sphere

We propose here to investigate the influence of the radiation pressure on the Hill sphere radius.

By definition, the Hill sphere of a planet/satellite (or also called the sphere of influence) is the region in which a light body stays under the gravitational influence of the planet/satellite. Because of the presence of a second heavy body, the gravitational influence of the planet/satellite is limited (e.g. star-planet or planet-satellite systems). This definition should not be mixed with the Roche lobe one which is the region limited by the furthest closed equipotential from the body and of which the shape is like a drop. The Roche lobe, in the case of $\beta = 0$ (no radiation pressure), passes through L_1 and near L_2 .

The Hill sphere radius is a first order approximation of the Lagrange L_1 and L_2 positions (L_1 and L_2 are approximatively at the same distance from the planet). Literally, the Roche lobe is inside the Hill sphere and have in common only one or two points, L_1 and/or L_2 . The radius of the Hill sphere is approximatively given at the first order by the value $R_{H0} = \sqrt[3]{\mu/3}$ (Hill, 1878) scaled by the star-planet (or planet-satellite) distance.

Following the demonstration for the Hill sphere radius R_H , if we take into account the radiation pressure (i.e. $\beta \neq 0$), then R_H - i.e. the position of the L_2 Lagrange point with respect to the lightest body - is given by the following relation:

$$\begin{aligned} -(1-\beta) \frac{1-\mu}{(1+R_H)^2} - \frac{\mu}{R_H^2} + (1-\mu+R_H) &= 0 \\ -(1-\beta)(1-\mu)R_H^2 & \\ -\mu(1+R_H)^2 + R_H^2(1+R_H)^2(1-\mu+R_H) &= 0 \end{aligned}$$

$$\begin{aligned} R_H^5 + (3-\mu)R_H^4 + (3-2\mu)R_H^3 & \\ + [\beta(1-\mu) - \mu]R_H^2 - 2\mu R_H - \mu &= 0 \end{aligned} \quad (2)$$

as presented in Simmons et al. (1985) (cf. Eq. (10) with $\delta_1^3 = 1 - \beta$ and $\delta_2^3 = 1$ in their paper).

According to Descartes' (1637) rule, this polynomial has only one positive root (because the sign between two successive monomials changes once), the Hill sphere radius. As we know, this polynomial does not have explicit roots (for polynomials with a higher degree than 4, the roots cannot be written explicitly as a function of coefficients, cf. the Abel–Ruffini theorem Abel, 1824). We can however reasonably assume that $R_H \ll 1$, $\mu \ll 1$ and $\mu \ll R_H$: according to Hill's formula (without radiation pressure), $R_H(\beta = 0) = O(\mu^{1/3})$; and according to Beth et al. (2016b), a large radiation pressure should lead to a Hill sphere radius located at $R_H(\beta) \approx \sqrt{\mu/\beta}$.

More precisely, Beth et al. (2016b) investigated the effect of radiation pressure superimposed to the gravity of the planet. In the CR3BP, it can be reasonably assumed that the centrifugal force is offset by the mass of the heaviest body in the system, in first approximation, so that only the planetary gravity and radiation pressure are not cancelled. In their paper, they showed that the bounded trajectories to the planet can be found until a limit distance called the exopause at $R_{pressure} = \sqrt{GM/a} = \sqrt{M_{pl}r_S^2/\beta M_S} \approx \sqrt{\mu/\beta} d_{pl}$, with a the acceleration induced by the radiation pressure at the planet's location, distant from the star at d_{pl} in any direction. The bounded particles could still be found in a sphere of radius $R_{pressure}$, further than the last closed equipotential.

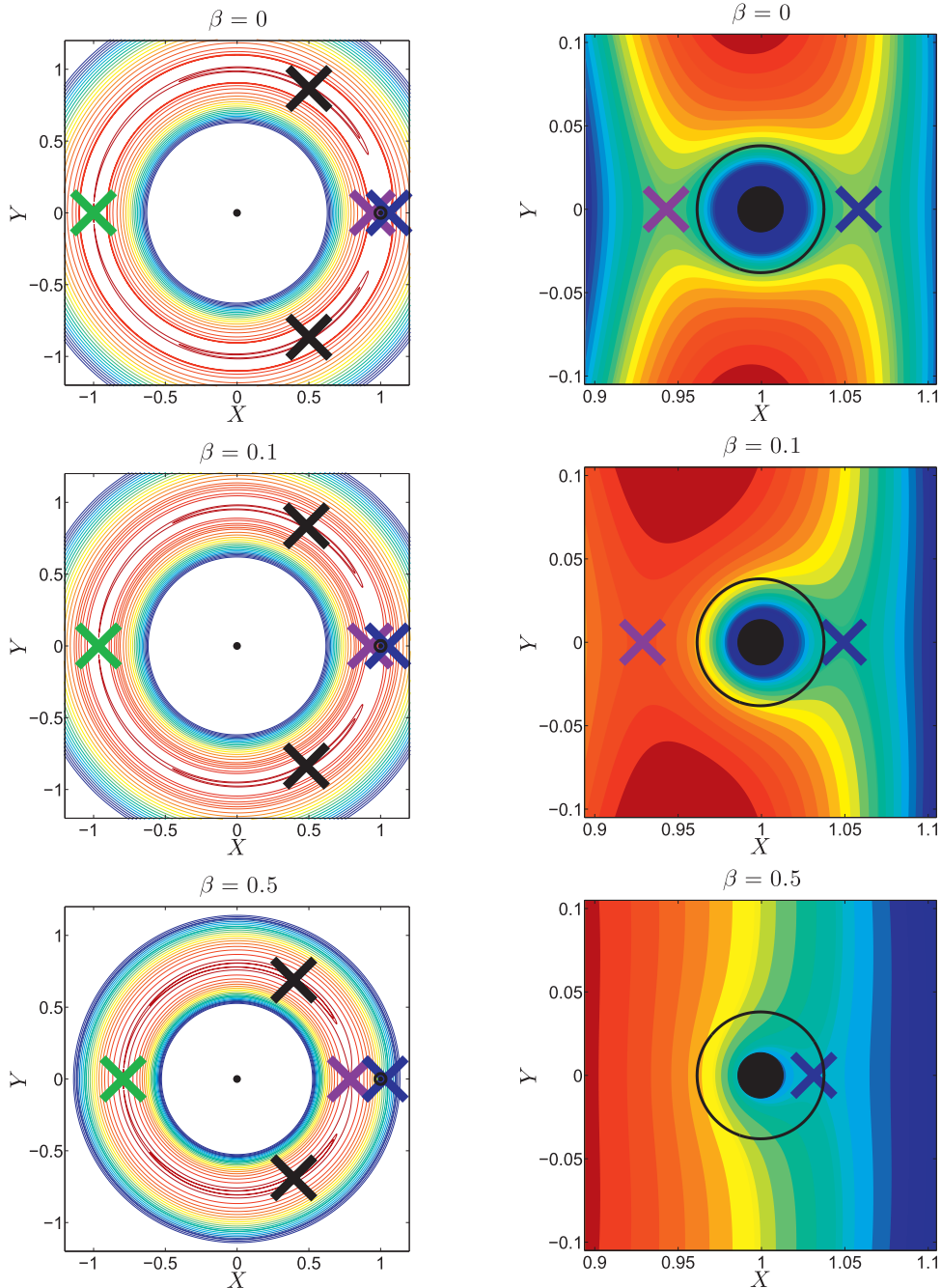


Fig. 2. Levels of effective potential Ω for $\beta = 0$ (pure CR3BP, upper panels), 0.1 and 0.5 for HD 209458b. The left panels provide a global picture of the equipotentials in the system and the right ones correspond to a zoom in the vicinity of HD 209458b. Warm/cold colors refer to high/low potential energies. The crosses define the Lagrange points: L_1 (violet), L_2 (blue), L_3 (green), L_4 and L_5 (black). The central point corresponds to the star position. The black point around $(1 - \mu, 0)$ corresponds to the true planetary size and the surrounding black circle to the exobase with its supposed size. (For interpretation of the references to color in this figure legend, the reader is referred to the web version of this article.)

We thus cut the relation 2 at the first power not depending on β which is R_H^3 (for the initial derivation of the Hill sphere radius, only the terms R_H^3 and $O(1)$ are kept). Thus, the relation 3.2 gives us:

$$3R_H^3 + \beta R_H^2 - \mu \approx 0 \quad (3)$$

This polynomial has one positive root and two negative (if $\beta > 9\sqrt[3]{\mu/12}$) or complex conjugates (if $\beta < 9\sqrt[3]{\mu/12}$) roots. The value of the generalized Hill sphere radius $R_H(\beta)$ is the positive root and

can be found analytically thanks to the Cardano method:

$$R_H(\beta) = \frac{\beta}{9} \left[2 \cosh \left(\frac{1}{3} \operatorname{argcosh} \left(\frac{1}{2} \left(\frac{9R_{H0}}{\beta} \right)^3 - 1 \right) \right) - 1 \right] \quad (4)$$

for $\beta < 3\sqrt[3]{9\mu/4}$,

$$R_H(\beta) = \frac{\beta}{9} \left[2 \cos \left(\frac{1}{3} \arccos \left(\frac{1}{2} \left(\frac{9R_{H0}}{\beta} \right)^3 - 1 \right) \right) - 1 \right] \quad (5)$$

for $\beta > 3\sqrt[3]{9\mu/4}$ with $R_{H0} = R_H(0) = \sqrt[3]{\mu/3}$ the well-known Hill sphere radius without radiation pressure.

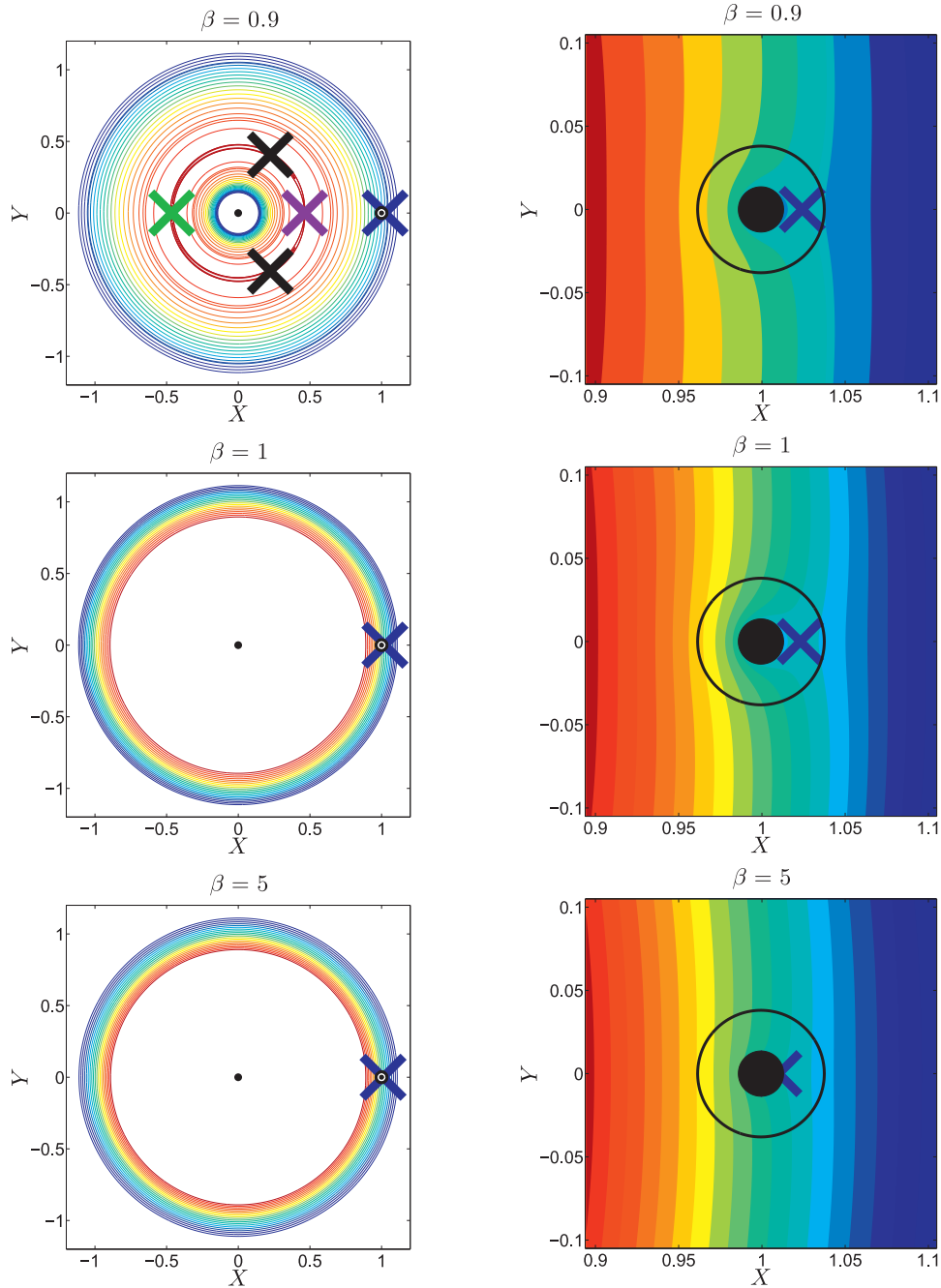


Fig. 3. Same as Fig. 2 for $\beta = 0.9, 1$ and 5 for HD 209458b.

The upper panel of Fig. 4 shows the evolution of the Hill sphere size as a function of μ and β . The planetary systems with low mass planet/star mass ratios are thus more sensitive to the radiation pressure (in particular at low β values, i.e. from 0 to 0.5), with a Hill sphere radius decreasing more rapidly when the radiation pressure (β) increases.

To justify the use of this convenient formula, we compare our analytical solution of Eq. (3) with the solution obtained numerically from Eq. (2) (see Fig. 4, middle panel). Our analytical formula thus approximates the position of L_2 with only $\sim 3\%$ error for $\mu = 10^{-3}$ (case of the Sun–Jupiter system). Moreover, this error decreases quickly with μ decreasing.

The Taylor series of our analytical formula gives:

- for $\beta \ll 1$: $R_H(\beta) = \sqrt[3]{\frac{\mu}{3}} \left(1 - \frac{\beta}{9} \right) + o(\beta)$

- for $\beta \gg 1$: $R_H(\beta) = \sqrt[2]{\frac{\mu}{\beta}} - \frac{\mu}{12\beta^2} + o(\beta^{-2})$

The $\beta = 0$ asymptote corresponds to the classical Hill sphere radius without radiation pressure, whereas the $\beta \rightarrow +\infty$ asymptote corresponds to the exopause distance induced by the radiation pressure and discussed in detail by Beth et al. (2016b). Our generalized Hill sphere radius thus provides the location of the Hill sphere radius for any regime of the stellar radiation pressure. Moreover, this gives a mathematical basis the exopause induced by the radiation pressure, introduced by Bishop (1991) and later numerically demonstrated by Beth et al. (2016b). The generalized formula is all the more interesting since the asymptotic values can be used for restricted conditions of the radiation pressure. For an error below $\sim 1\%$, the first asymptote (i.e. the classical Hill sphere

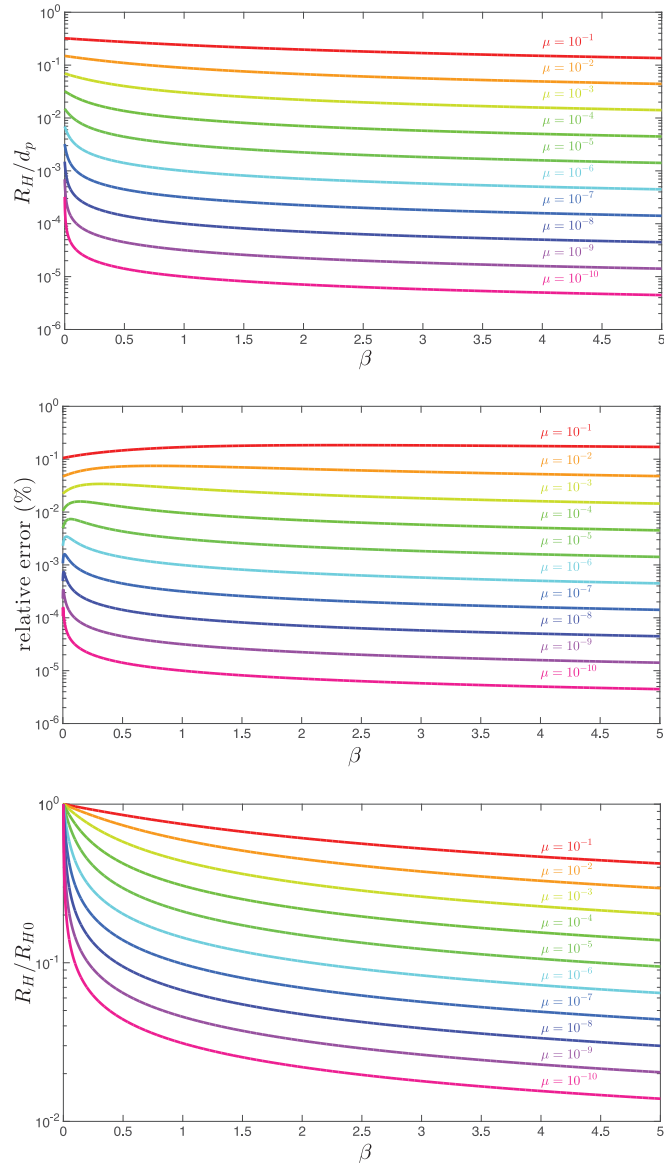


Fig. 4. (Upper panel) Ratio between the generalized Hill sphere radius and the planet-star distance as a function of β . (Middle panel) Relative difference between the exact numerical root from Eq. (2) and our analytical solution from Eq. (3). (Lower panel) Same as upper panel, with the modified Hill sphere radius scaled with the Hill sphere radius for $\beta = 0$ (pure CR3BP), for different μ values. For $\beta = 0$, we have the usual value of the Hill sphere radius $\sqrt[3]{\mu/3}$ without radiation pressure. For higher β , the modified Hill sphere radius converges asymptotically to $\sqrt{\mu/\beta}$, i.e. the exopause distance discussed by Beth et al. (2016b).

radius) is valid until $\beta \approx 0.1R_{H0}$ only, whereas the second asymptote (i.e. the exopause distance) is valid only above $\beta \approx 36R_{H0}$.

The β parameter depends both on the stellar photon flux at each wavelength and on the species considered. This work investigates only the radiation pressure effect on Hydrogen atoms but for further studies, other species such as Helium should be investigated too. In Table 1, we provide the modified Hill sphere radius in planetary radii for Venus, Earth, Mars, HD 209458b and GJ 436b for various typical β values. In the current Solar System, for Hydrogen, β is between 0.4 and 1.4 with daily variations (Vidal-Madjar, 1975). The first column (i.e. $\beta = 0$) references the Hill sphere radius in planetary radii as used in literature. With the effect of the radiation pressure, the size of the Hill sphere may decrease strongly depending on the mass, the distance to the star and the radiation pressure (β). For example, the size of the Hill sphere decreases by

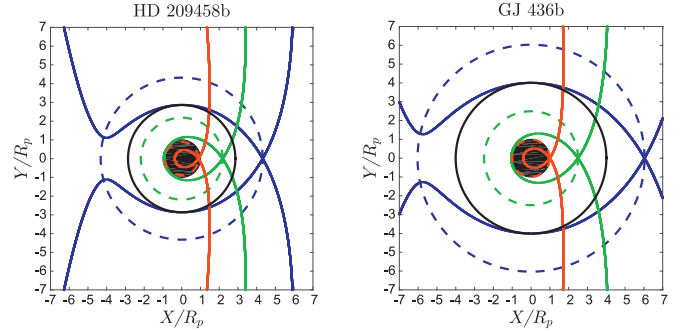


Fig. 5. Equipotentials around HD 209458b (left) and GJ 436b (right) for different radiation pressure intensities: $\beta = 0$ (blue), 0.6 (green; nominal case for GJ 436b) and 4 (red; nominal case for HD 209458b). The corresponding Hill sphere is the circle in dotted line with the corresponding color. The filled centered circle corresponds to the solid core of the planet and the black solid circle to the circle bordered by the Roche lobe often assimilated to the top of the dense atmosphere or to the exobase. (For interpretation of the references to color in this figure legend, the reader is referred to the web version of this article.)

a factor of 6.6/6.3/9.2 for Venus/Earth/Mars when $\beta = 1.2$ (maximum radiation pressure) is considered instead of $\beta = 0$ (no radiation pressure). The case of HD 209458b is also quite interesting: according to Bourrier and Lecavelier des Etangs (2013), the β value for HD 209458b should be ~ 4 , neglecting relativistic effects and absorption (i.e. the shadowing effect), and thus the Hill sphere radius should be below the surface according to our study. A similar study is performed for GJ 436b: its characteristic are derived by Southworth (2010) for the planet and by Torres (2007) for the star (see http://exoplanet.eu/catalog/gj_436_b/). For this warm Neptune-like planet, μ is $\approx 1.48 \cdot 10^{-4}$ and $\beta \sim 0.6$ for low radial velocities ($v \approx 0$) of Hydrogen atoms (Bourrier et al., 2015). This other case study shows a similar behavior as HD 209458b with a strong decrease of the modified Hill sphere, even if β is lower.

We can also investigate the conditions encountered by the early Solar System. The Lyman- α intensity was 20 times higher for the one million year old Sun than at present (Lammer et al., 2013), leading to an estimated β for Hydrogen of about 20. If we assume the planets were in the same place as today, the sphere of influence should be much closer to the planetary surface, at only some planetary radii (less than 10).

The consequences on the atmospheric stability and escape flux, in particular for the case studies HD 209458b and GJ 436b, will be more detailed in the Sections 3.3 and 3.4.

3.3. Consequences on the stability of planetary atmospheres

Regarding the example of the hot Jupiter HD 209458b, Lecavelier des Etangs et al. (2004) proposed that the exobase of the planet is shaped by the Roche lobe proximity, since the L_1 Lagrange point is expected to be close to the planet due to the close host star. This then induces a geometrical blow-off: the exospheric particles need much less kinetic/thermal energy to escape by reaching the close Roche lobe. Based on our analysis, we agree in this case with the geometrical blow-off of HD 209458b proposed by Lecavelier des Etangs et al. (2004) but for a different reason: as can be seen in Fig. 5 (left panel), the radiation pressure (with $\beta \approx 4$ according to Bourrier and Lecavelier des Etangs, 2013) pushes the position of the Roche lobe (i.e. L_1) much closer to the star and thus much further away from the planet, but the L_2 point is pushed closer to the planet below the expected exobase location (and even below the “surface”), so that no kinetic/thermal energy is needed for exospheric particles to escape even for a low exospheric temperature.

Table 1

Modified Hill sphere radius in planetary radii with the effect of the radiation pressure for different planets (Venus, Mars, Earth, HD 209458b and GJ 436b) and for different β values (0,0.4,0.6,1.4,2,4,20). The classical Hill sphere radius (without radiation pressure) corresponds to $\beta = 0$.

Planets	$\beta = 0$	$\beta = 0.4$	$\beta = 0.6$	$\beta = 1.4$	$\beta = 2$	$\beta = 4$	$\beta = 20$
Venus	167.5	43.91	35.99	23.62	19.78	13.99	6.25
Earth	235.7	63.87	52.36	34.39	28.78	20.36	9.10
Mars	320.2	60.24	49.25	32.28	27.01	19.10	8.54
HD 209458b	4.32	2.56	2.18	1.49	1.25	0.89	0.40
GJ 436b	6.23	3.12	2.61	1.75	1.47	1.04	0.47

A similar study was performed on the warm Neptune-like exoplanet, GJ 436b, observed and studied by [Ehrenreich et al. \(2015\)](#) and further by [Bourrier et al. \(2015\)](#). They highlight an unusual structure of the exosphere: a comet-like shape. According to [Bourrier et al. \(2015\)](#), β is around 0.6 for small velocities. Thus, we plot in [Fig 5](#), right panel, the corresponding equipotential in green passing through L_2 and the corresponding Hill sphere. Like for HD 209458b, the radiation pressure reduces the Roche lobe and is located below the exobase, assuming an optically thin atmosphere at any altitude.

As mentioned above the early Solar System planetary atmospheres encountered a Lyman- α flux about 20 times higher than today ([Lammer et al., 2013](#)) and leading to a β value of the order of 20 instead of 0.4–1.4. Consequently, assuming the distance of Venus, Earth and Mars were the same as today, the sphere of influence for Hydrogen should be of the order of 6 and 9 planetary radii. The radiation pressure thus strongly limited the possible extension of the atmosphere: above this limit, Hydrogen (and species with similar β) could not be bounded to the planet by the gravity and easily escaped to the interplanetary medium. This radiation pressure effect is a new constraint for understanding the planetary atmospheres evolution in the solar or exoplanetary systems as well as for their modeling: the size of the simulation box should thus be at least larger than the Hill sphere radius of each species to appropriately take into account the radiation pressure effect.

In the aim to have a complete picture of the atmospheric evolution of planets, which includes the influence of the radiation pressure, one should not only take into account the evolution of the stellar EUV-XUV fluxes that drive the heating/expansion of the atmospheres, but also the part of the flux spectrum that drives the radiation pressure. Depending on the flux spectrum of the host star, the species inside the atmosphere will be more or less affected by the radiation pressure based on their specific β value. For example, if we refer to [Chamberlain and Hunten \(1987\)](#) for the Solar System conditions, the β parameter of Helium can be between 0 or very small values (e.g. 0.06 for He II) and 260 depending on the wavelength. If several species are not equally sensitive to the stellar radiation pressure, this could then affect the dynamic of each species above the exobase and yield to a differential drag of the species in the upper atmosphere, or to a protection of (radiation pressure) sensitive species such as Hydrogen by less sensitive ones through collisions. This last process could help understanding how Hydrogen rich atmospheres can remain stable for long periods despite a blow-off type escape regime expected. These questions will be investigated in a future work.

Moreover, it can be reasonably assumed that the radiation pressure will have a different effect on planetary atmospheres according to the Knudsen number Kn :

- for $Kn \ll 1$ (collisional regime), i.e. the scale height is greater than the mean free path, the radiation pressure will increase the mechanical energy of each Hydrogen atom on short distances similar to the mean free path. Then, through collisions, this increase will be redistributed quickly to other species and

converted into heat. The escaping flux will be a function of the incoming UV flux and its heating efficiency,

- for $Kn \gg 1$ (collisionless regime), i.e. the mean free path is higher than the scale height, the radiation pressure will affect only the dynamics of each individual species on time scale shorter than $1/\nu$, ν the collisional frequency. The escaping flux will be function of the radiation pressure and the local thermal speed.

3.4. Escaping flux: the case studies HD 209458b and GJ 346b

As detailed above (and seen in [Table 1](#)), the cases of interest HD 209458b GJ 436b have their Hill sphere radii (or exopause) below the exobase if we assume an optically thin atmosphere. Under the assumption that the atmosphere is optically thin until the exobase (see [Section 4](#)), an exopause below the exobase implies that, all particles at the exobase thus escape (see [Beth et al., 2016b](#)). This means the escape velocity is “virtually” reduced to 0 and thus the Jeans’ parameter $\lambda_c = v_{esc}^2/v_{th}^2$ (v_{esc} and v_{th} being the escape and thermal speed) tends to 0. The critical Jeans’ parameter for the hydrodynamical blow-off regime proposed by [Hunten \(1982\)](#) is 2, but with the additional effect of the radiation pressure, λ_c will reach even lower values. The thermal escape flux may then be given by the Jeans’ escape formula \mathcal{F}_j ([Jeans, 1916](#)) applied to the exobase directly illuminated (i.e. the half of the planet) with $\lambda_c = 0$, which leads for Hydrogen at HD 209458b to the following mass loss rate:

$$\dot{M} = 2\pi r_{exo}^2 n_{exo} m_{\mathcal{F}_j}(\lambda_c = 0) = n_{exo} r_{exo}^2 \sqrt{2\pi m_H k_B T_{exo}} \approx 2.5 \cdot 10^{10} \text{ g s}^{-1} \quad (6)$$

for a temperature T_{exo} of 8000 K, an exobase at a distance of 2.8 planetary radii and a density at the exobase of the order of 10^{13} m^{-3} ([Bourrier and Lecavelier des Etangs, 2013](#); [Lecavelier des Etangs et al., 2004](#)). This loss rate is in agreement with the estimates by [Vidal-Madjar and Lecavelier des Etangs \(2004\)](#), i.e. above 10^9 g s^{-1} , and of the same order as recent models which predict a range of loss rates between 10^9 and 10^{11} g s^{-1} ([Koskinen et al., 2013](#)). However, the exobase temperature is poorly known and could be much lower than the one used by [Lecavelier des Etangs et al. \(2004\)](#) to match their model with the spectroscopic observations. Then, we have performed as well the same calculation with the effective temperature of HD 209458b which is $T_{eff} \sim 1400 \text{ K}$ ([Charbonneau et al., 2000](#); [Evans et al., 2015](#)). Assuming the same order of magnitude for the density at the exobase than previously assumed, we obtain $\dot{M} \approx 10^{10} \text{ g s}^{-1}$, to be compared with the classical Jeans’ escape, which is here of about $\dot{M} \sim 20 \text{ g s}^{-1}$. Thus, extreme temperatures (compared with T_{eff}) are not required to obtain a good agreement with the observed mass loss rates for HD 209458b.

The same approach can be applied to GJ 436b as well. Nevertheless, two information are missing from the literature: the height of the exobase and its temperature. Recently, [Bourrier et al. \(2015\)](#) modeled the structure of the exosphere around GJ 436b and its cometary-like shape. The distance from the planet where they

released the particles for their simulation is the Roche lobe radius assuming an hydrostatic profile below. Nevertheless, they admit that the Knudsen number is already around 40 at this altitude and thus the exobase is below. If we assume that the scale height is a function of only gravity (i.e. with a constant temperature fixed at 717 K Demory et al., 2007), one can find an exobase height at around ~ 3.1 planetary radii (this value is lower for higher temperatures) leading to the following escaping rate:

$$\dot{M} = n_{\text{exo}} r_{\text{exo}}^2 \sqrt{2\pi m_{\text{H}} k_{\text{B}} T_{\text{exo}}} \approx 6.9 \cdot 10^7 - 10^8 \text{ g} \cdot \text{s}^{-1} \quad (7)$$

with a density at $3.1 R_{\text{p}}$ between 10^{12} and 10^{13} m^{-3} (Guo and Ben-Jaffel, 2016). This result is in agreement with the escape rate derived from observations (Ehrenreich et al., 2015). We thus obtain similar escape rates to previous models, but with a different process, i.e. with a geometrical “blow-off” due to the radiation pressure influence and not due to the Roche lobe proximity. Furthermore, for hot Jupiters, the thermal escape or Jeans’ escape is in the literature neglected but our study shows that the radiation pressure acceleration modifies the gravitational potential in such a way that the exospheric particles are not bounded any more and/or the Jeans’ parameter tends to 0. Thus, the thermal escape is strongly enhanced by the stellar radiation pressure, favoring the escape of exospheric particles.

4. Discussion and limits of this approach

In this section, we list and discuss the assumptions and limits of the approach used in this paper. The current results are not meant to replace a full 3D kinetic model of the corona of the planet/exoplanet. However, our approach still provides valuable results to investigate the influence of the radiation pressure and the stellar gravity. In particular, our results are appropriate for the field of comparative planetology.

The assumptions are:

- the Doppler shift and the relativistic effects are neglected, that is that the radiation pressure is assumed to depend only on the position.
- the Coriolis effect is neglected as well because it is depending on the velocity of the particle. Even if this is a conservative force, the associated potential is a function of the velocity unfortunately. This assumption combined with the previous ones allowed us to study the potential energy acting on the particle.
- the optical depth of the line of interest (for this study, the Lyman- α line) is supposed less than one at the exobase. This means that we neglect the self-shielding effect from the dayside corona on the dayside exobase. This assumption is discussed further below.

The assumption of a thin atmosphere at the exobase level on the dayside may be invalid. France et al. (2010) reported large column densities for HD 209458b, and Bourrier and Lecavelier des Etangs (2013) revealed strong absorption effects based on 3D kinetic simulations. A strong absorption due to a thick atmosphere above the exobase would reduce the radiation pressure influence and thus impact the results discussed here. However, several points can be raised to discuss the validity of this assumption, which show that detailed investigations would be needed to provide definitive conclusions, and that the radiation pressure most probably influences both the equipotentials and atmospheric escape of hot Jupiters.

First, as this is not possible to perform dayside observations, the informations (atmospheric characteristics, i.e. temperature, density, etc.) which we are interested in come from other modeling works. However, the current photochemical models (based on the flux conservation) for the low atmosphere assume a spherical symmetry (1D), with or without tidal forces, are run further than the

exobase (whereas above this limit, the fluid approach is inaccurate) and generalized their density profiles in any direction.

Even if we neglect the radiation pressure, the approximation for the tidal forces are not fulfilled at all in the perpendicular plane to the star-planet direction. Moreover, the 1D assumption cannot be reliable above the exobase where the dynamic of the particles is mainly determined by external forces: the Coriolis force could be particularly strong for Hot Jupiter systems and leads to an acceleration in the Y direction if the particles are presumed moving along the X-axis (1D case) only.

Only kinetic approaches, such as performed by Bourrier and Lecavelier des Etangs (2013), could be accurate above the supposed exobase height. However, the optical thickness provided by the transit observations (and reproduced by numerical models) include the strong contribution of the lower atmosphere, leading an optically thick atmosphere along the line of sight from the star to the observer. In our case, we only need the atmosphere to be optically thin until the exobase (excluding the lower atmosphere).

Another interesting point is the asymptotic formula for β_c , the critical value for which the Roche lobe of the star and the planet are not connected any more. Applied to our case studies, the critical β values are $3.31 \cdot 10^{-3}$ for HD 209458b and $1.34 \cdot 10^{-3}$ for GJ 436b. This means if an atom is subject to a relative β (eventually reduced by the optical depth) above these critical values, the particle will escape more easily through L_2 than L_1 . Let us assume a simple attenuation of the beta value due to the optical depth τ between the particle and the star, such as $\beta(\tau) = \beta_{\infty} \exp(-\tau)$ where β_{∞} is β in absence of atmosphere (respectively 4 and 0.6 for HD 209458b and GJ 436b). If we look for τ_c such as $\beta(\tau_c) = \beta_c$, one obtains 7.1 for HD 209458b and 6.1 for GJ 436b. Thus, for any shell of the atmosphere with optical depths lower than these limits for each planet, the particles are still very sensitive to the radiation pressure. The influence of the radiation pressure on the equipotentials and on the atmospheric escape thus cannot be neglected even if the optical thickness is above 1.

In addition, one can note that the above expression for the β attenuation assumes a pure absorption of the photons, whereas they can also be scattered (resonant scattering, scattering or (absorption+emission)), thus needing a radiative transfer model to rigorously assess the effect of the radiation pressure in the corona for optically thick parts. Debout et al. (2016) for example showed that near the nucleus of comet 67P, some regions have a g-factor (proportional to the radiation pressure) higher than the value in optically thin parts, due to resonant scattering of photons by H_2O .

Finally, it is interesting to note that, beyond the uncertainties due to the shadowing effect, and as shown by Fig. 6, the radiation pressure enhances the asymmetry between the dayside and the nightside by moving L_1 away from the planet and L_2 toward, even for small β and μ values.

5. Conclusions

In this paper, we show the effect of the radiation pressure on the Circular Restricted Three Body Problem (CR3BP). This problem was previously tackled for Celestial Mechanics purposes but rarely in the context of Planetary Sciences.

We first discuss the influence of the radiation pressure on the positions of the Lagrange points, before we derive for the first time an analytical formula to approximate the Hill sphere radius with the additional effect of the radiation pressure. We highlight the strong interest of this derivation for the case studies of exoplanets and in particular for hot Jupiters. Most of the papers dealing with the Hill sphere (or Roche lobe) and the stability of Hot Jupiters atmospheres do not take account the effect of the radiation pressure on the CR3BP but only tidal effects.

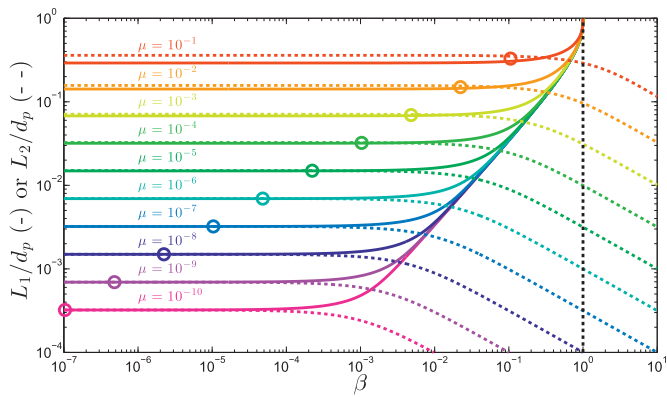


Fig. 6. Relative distances of L_1 and L_2 in planet-star distance (d_p) for different values of μ . The solid lines correspond to the L_1 position for a given μ and the dashed lines to L_2 . The circles correspond to the $\beta_c(\mu)$ value for which the L_1 and L_2 have the same potential: for $\beta > \beta_c(\mu)$ as defined by the circle, this is easier for a particle to escape through L_2 than L_1 . The horizontal line at $\beta = 1$ is the limit from which L_1 does not exist any more.

We show in extreme cases such as for hot Jupiters like HD 209458b or warm Neptune like GJ 436b that the Hill sphere radius could be drastically reduced and even be located below the surface. The components of the upper atmosphere, which are sensitive to the radiation pressure, are thus not “bounded” to the planet any more and then escape to the interplanetary medium. The resulting increased escapes calculated for HD 209458b and GJ 436b are in agreement with the observations. Moreover, we show that our two case studies are in a “blow-off” type escape regime due to the radiation pressure of the host star, in contradiction with previous works that considered a blow-off regime due to the proximity of the Roche lobe (the Lagrange point L_1 being actually pushed toward the star by the radiation pressure, the escape is then much easier through L_2 than L_1). Thus, the radiation pressure can modify the planetary escape flux and strongly affect the atmospheric evolution of hot Jupiter and/or warm Neptune atmospheres from their early age, depending on the evolution of the host star as well and those of terrestrial planets. Other exoplanets could be targets of interest to apply our approach when more information (data and models) on the upper atmosphere and the exobase will be available.

Some assumptions are done in this work (e.g. neglecting relativistic effects and the shadowing effect of the planet and its atmosphere), which may change the quantitative results given in the paper. Full 3D Monte Carlo simulations including the radiation pressure and a radiative transfer model will be needed to derive realistic results. However, these investigations will be dependent on the planet and our work proposes a simplified global picture in order to provide clues for comparative planetology and better understand the specific influence of the radiation pressure force on the equipotentials and atmospheric escape.

In a future work, we will investigate the influence of the self-shadowing effect on the radiation pressure intensity in the vicinity of the planets, and analyze how the intense radiation pressure of the young Sun may have influenced the atmospheric escape and evolution of the inner Solar System planets, whose Hill sphere radii were significantly reduced.

Acknowledgments

This work was supported by the Centre National d’Études Spatiales (CNES) and by the STFC of UK under Grants ST/K001051/1 and ST/N000692/1.

References

- Abel, N. H., 1824. Mémoire sur les équations algébriques, où on démontre l'impossibilité de la résolution de l'équation générale du cinquième degré.
- Beth, A., Garnier, P., Toubanc, D., et al., 2016. Theory for planetary exospheres: I. Radiation pressure effect on dynamical trajectories. *Icarus* 266, 410–422.
- Beth, A., Garnier, P., Toubanc, D., et al., 2016. Theory for planetary exospheres: II. Radiation pressure effect on exospheric density profiles. *Icarus* 266, 423–432.
- Bishop, J., 1991. Analytic exosphere models for geocoronal applications. *Planet. Space Sci.* 39, 885–893.
- Bishop, J., Chamberlain, J.W., 1989. Radiation pressure dynamics in planetary exospheres: A natural framework. *Icarus* 81, 145–163.
- Bourrier, V., Ehrenreich, D., Lecavelier des Etangs, A., 2015. Radiative braking in the extended exosphere of GJ 436 b. *Astron. Astrophys.* 582, A65.
- Bourrier, V., Lecavelier des Etangs, A., 2013. 3D model of hydrogen atmospheric escape from HD 209458b and HD 189733b: Radiative blow-out and stellar wind interactions. *Astron. Astrophys.* 557, A124.
- Burns, J.A., Lamy, P.L., Soter, S., 1979. Radiation forces on small particles in the Solar System. *Icarus* 40, 1–48.
- Chamberlain, T.P., Hunten, D.M., 1987. Theory of planetary atmospheres: An introduction to their physics and chemistry. International Geophysics. Elsevier Science.
- Charbonneau, D., Brown, T.M., Latham, D.W., et al., 2000. Detection of planetary transits across a Sun-like star. *Astrophys. J.* 529, L45.
- Debout, V., Bockele Morvan, D., Zakharov, V., 2016. A radiative transfer model to treat infrared molecular excitation in cometary atmospheres. *Icarus* 265, 110–124.
- Demory, B.O., Gillon, M., Barman, T., et al., 2007. Characterization of the hot Neptune GJ 436 b with spitzer and ground-based observations. *Astron. Astrophys.* 475, 1125–1129.
- Descartes, R., 1637. La Géométrie, appendix to Discours de la méthode.
- Ehrenreich, D., Bourrier, V., Wheatley, P.J., et al., 2015. A giant comet-like cloud of hydrogen escaping the warm Neptune-mass exoplanet GJ 436b. *Nature* 522, 459–461.
- Erkaev, N.V., Kulikov, Y.N., Lammer, H., et al., 2007. Roche lobe effects on the atmospheric loss from aa hot Jupiters. *Astron. Astrophys.* 472, 329–334.
- Lecavelier des Etangs, A., Vidal-Madjar, A., McConnell, J.C., et al., 2004. Atmospheric escape from hot Jupiters. *Astron. Astrophys.* 418, L1–L4.
- Evans, T.M., Aigrain, S., Gibson, N., et al., 2015. A uniform analysis of HD 209458b spitzer/IRAC light curves with gaussian process models. *Mon. Not. R. Astron. Soc.* 451, 680–694.
- Ferziger, J., Kaper, H., 1972. Mathematical Theory of Transport Processes in Gases. North-Holland Publishers.
- France, K., Stocke, J.T., Yang, H., et al., 2010. Searching for far-ultraviolet auroral/dayglow emission from HD 209458b. *Astrophys. J.* 712, 1277.
- Garcá Muñoz, A., 2007. Physical and chemical aeronomy of HD 209458b. *Planet. Space Sci.* 55, 1426–1455.
- Guo, J.H., Ben-Jaffel, L., 2016. The influence of the extreme ultraviolet spectral energy distribution on the structure and composition of the upper atmosphere of exoplanets. *Astrophys. J.* 818, 107.
- Hill, G.W., 1878. Researches in the lunar theory. *Am. J. Math.* 1, 5–26.
- Hunten, D.M., 1982. Thermal and nonthermal escape mechanisms for terrestrial bodies. *Planet. Space Sci.* 30, 773–783.
- Jean, J.H., 1916. The Dynamical Theory of Gases, fourth ed. Cambridge University Press. 1925
- Koskinen, T., Yelle, R., Harris, M., et al., 2013. The escape of heavy atoms from the ionosphere of HD209458b. II. Interpretation of the observations. *Icarus* 226, 1695–1708.
- Lammer, H., Kislyakova, K., Gdel, M., 2013. Stability of Earth-Like N_2 atmospheres: Implications for habitability. In: Trigo-Rodríguez, J., Raulin, F., Müller, C., Nixon, C. (Eds.), The Early Evolution of the Atmospheres of Terrestrial Planets (Astrophysics and Space Science Proceedings), 35. Springer New York, pp. 33–52.
- Phillips, S.N., Podsiadlowski, P., 2002. Irradiation pressure effects in close binary systems. *Mon. Not. R. Astron. Soc.* 337, 431–444.
- Schuerman, D.W., 1972. Roche potentials including radiation effects. *Astrophys. Space Sci.* 19, 351–358.
- Schuerman, D.W., 1980. The restricted three-body problem including radiation pressure. *Astrophys. J.* 238, 337–342.
- Simmons, J., McDonald, A., Brown, J., 1985. The restricted 3-body problem with radiation pressure. *Celest. Mech.* 35, 145–187.
- Southworth, J., 2010. Homogeneous studies of transiting extrasolar planets III. Additional planets and stellar models. *Mon. Not. R. Astron. Soc.* 408, 1689–1713.
- Torres, G., 2007. The transiting exoplanet host star GJ 436: A test of stellar evolution models in the lower main sequence, and revised planetary parameters. *Astrophys. J.* 671, L65.
- Vidal-Madjar, A., 1975. Evolution of the solar Lyman- α flux during four consecutive years. *Sol. Phys.* 40, 69–86.
- Vidal-Madjar, A., Lecavelier des Etangs, A., 2004. “Osiris” (HD209458b), an evaporating planet. In: Beaulieu, J., Lecavelier Des Etangs, A., Terquem, C. (Eds.), Extrasolar Planets: Today and Tomorrow. Astronomical Society of the Pacific, p. 152.
- Vidal-Madjar, A., des Etangs, A.L., Desert, J.M., et al., 2003. An extended upper atmosphere around the extrasolar planet HD209458b. *Nature* 422, 143–146.
- Wang, J., Ford, E.B., 2011. On the eccentricity distribution of short-period single-planet systems. *Mon. Not. R. Astron. Soc.* 418, 1822–1833.
- Yelle, R., Helmut, L., Ip, W.H., 2008. Aeronomy of extra-solar giant planets. *Space Sci. Rev.* 139, 437–451.